S-72.333

Postgraduate Course in Radiocommunications

Fall 2000

Channel modeling

Dmitri Foursov
Communications Laboratory, HUT
Dmitri.Foursov@hut.fi

Content:

1. Introduction

Fading and Multipath occur in many radio communication systems. These effect were first observed and analyzed in troposcatter systems in the 50s and early 60s. In any wireless communication system there could be more than one path over which the signal can travel between the transmitter and receiver antennas.

The presence of multiple paths is due to atmospheric scattering and refraction, or reflections from buildings and other objects.

Multipath fading affects the signal in two ways: dispersion (time spreading or frequency selectivity) and time-variant behavior.

Mobile communications is affected, in addition to multipath (or small-scale fading), to another type of fading, which is referred to as shadow or large-scale fading. Shadow fading reveals itself as an attenuation of the average signal power. Shadow fading is induced by prominent terrain contours (hills, buildings, etc.) between transmitter and receiver.

A mobile wireless moving over a large area encounters both types of fading: multipath fading superimposed on the much slower fading. Thus, the mobile channel impulse response in its complex-lowpass equivalent form is composed of two components:

$$\tilde{h}(t,t) = s(t) \times \tilde{c}(t,t)$$

where $s(t)$ is the shadow fading component and $\tilde{c}(t,t)$ is the multipath component.

2. Shadow fading

The signal received by a mobile radio from a transmitter can be represented as

$$S_r = S_t + G_t + G_r - L_p$$

where S_r is the received signal in dBm, S_t is the transmitted signal in dBm, G_t is the transmit antenna gain toward the receiver in dB, G_r is the receive antenna gain toward the transmitter in dB and L_p is the propagation loss in dB.

The most difficult of these parameters to predict is the propagation loss L_p. Many models have been developed to try and predict this value. Currently, the most popular site-specific methods include ray-tracing techniques. These techniques were originally developed for indoor environment and have been extended to dense urban outdoor areas.

The most popular of the statistical propagation models are the class of slope-intercept models. These models treat the propagation loss as being comprised of a distance-related deterministic component as well as statistical components both for the shadow and multipath. The deterministic component is taken to be of the form

$$L_p = a + b \log_{10}(R) \qquad \text{[dB]}$$

where R is the distance between the transmitter and receiver in km and α and β are parameters determined by the model. Values for the parameters α and β can be determined from experimental measurements of specific radio system. Measurements are taken of received signal power averaged over several wavelengths, so that multipath effects are averaged out at many different locations around transmitter.

One of the first popular slope-intercept models was the Hata model. In the Hata model the slope parameter β depends on the height of the transmitter above the average ground elevation around it. The intercept parameter α depends on this height, the operating frequency, and the type of environment (rural, suburban, or urban) in which the mobile operating. These parameters are given by

$$b = 44.9 + 6.55 \log_{10}(h)$$

and the intercept

$$a = a_0 = 69.55 + 26.16 \log_{10}(f) - 13.82 \log_{10}(h) \qquad \text{urban environment}$$

$$a = a_0 - [2 \log_{10}^2 (f/28) + 5.4] \qquad \text{suburban environment}$$

$$a = a_0 - [4.78 \log_{10}^2 (f) - 18.33 \log_{10}(f) + 40.94] \qquad \text{rural environment}$$

where h is the transmitter height above average terrain elevation in meters, and f is the frequency in MHz.

The shadow fading statistical component of the slope intercept models can be determined by examining the residuals of the measurement data once the linear least squares fit to the log of the distance is removed. These residuals, in decibels, typically follow approximately a Gaussian distribution with a zero mean and a standard deviation of about 8 dB. Hence, the shadow fading component follows a log-normal distribution.

3. Multipath Fading

The multipath fading can be assigned into two categories:

1. The multipath signal paths are made up of a relatively small and identifiable number of components reflected by small hills, houses, and other structures encountered in open areas and rural environments. This results in a channel model with a finite number of multipath components. Such a channel is referred to as *discrete multipath channel*.

2. The multipath signal paths are generated by a large number of unresolvable reflections as might occur in a mountainous area or in a dense urban environment. This signal is composed of a continuum of unresolvable multipath components. This channel model is referred to as *diffuse multipath channel*.

3.1. Lowpass-Equivalent Characterization of Multipath Channels

A simple model for *discrete* multipath channel has the form

$$y(t) = \sum_n a_n(t)s(t - t_n(t))$$

where *s(t)* is the bandpass input signal, $a_n(t)$ is the attenuation factor for the signal received on the *n*th path, and $t_n(t)$ is the corresponding propagation delay. If we express *s(t)* as

$$s(t) = \mathrm{Re}\{\tilde{s}(t)e^{j2\pi f_c t}\}$$

then we can express the channel output

$$y(t) = \mathrm{Re}\left\{\left[\sum_n a_n(t)e^{-j2\pi f_c t_n(t)}\tilde{s}(t - t_n(t))\right]e^{j2\pi f_c t}\right\}$$

and the complex envelope of the output

$$\tilde{y}(t) = \sum_n a_n(t)e^{-j2\pi f_c t_n(t)}\tilde{s}(t - t_n(t)) = \sum_n \tilde{a}_n(t_n, t)\tilde{s}(t - t_n(t))$$

For the *diffuse* multipath channel the response is expressed in integral form as

$$\tilde{y}(t) = \int_{-\infty}^{\infty} \tilde{a}_n(t, t)\tilde{s}(t - t)dt$$

3.2. Statistical Characterization of Multipath Channels

The multipath fading for both the *diffuse* and *discrete* channels manifest itself in two effects:

1. Time spreading (in t) of the symbol duration within the signal, which is equivalent to filtering and bandlimiting.
2. A time-variant behavior (in *t*) of the channel due to motion of the receiver or changing environment such as movement of foliage or movement of reflectors and scatterers.

Figure 1 shows the consequences of both effects by showing the impulse response of the *diffuse* channel versus delay t at three instances of time *t*.

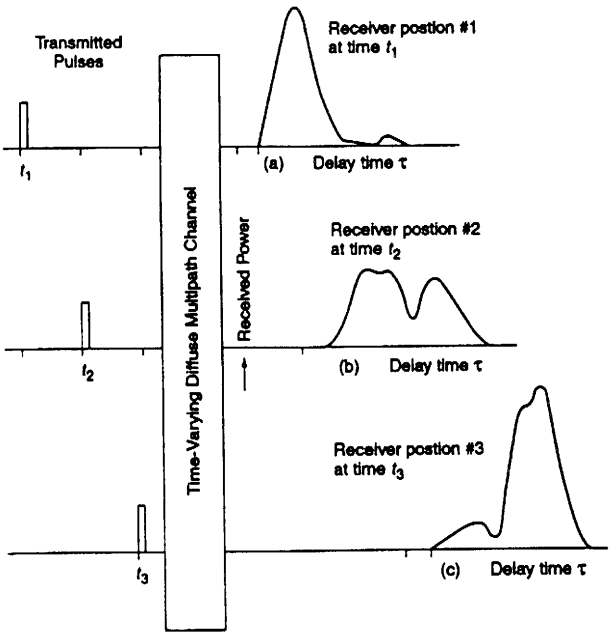

Fig. 1. The response to a narrow pulse versus delay at different receiver positions

3.3. Statistical Characterization of the Time-Variant Behavior

The random fluctuations in the received signal due to fading can be modeled by treating $\tilde{c}(t,t)$ as a random process in *t*. Since the components of the multipath signal arise from a large number of reflections and scattering from rough or granular surfaces, then by virtue of the central limit theorem, $\tilde{c}(t,t)$ can be modeled as a complex Gaussian process.

If $\tilde{c}(t,t)$ has a zero mean, then the envelope $R(t,t)=|\tilde{c}(t,t)|$ has a Rayleigh probability density function

$$f_R(r)=\frac{r}{s^2}e^{-r^2/(2s^2)}$$

If $\tilde{c}(t,t)$ has a nonzero mean, which implies the presence of a significant specular (nonfaded) line-of-sight component, then $R(t,t)=|\tilde{c}(t,t)|$ has a Ricean probability density function

$$f_R(r)=\frac{r}{s^2}I_0\left[\frac{Ar}{s^2}\right]e^{-(r^2+A^2)/(2s^2)}$$

where *A* is the nonzero mean of $\tilde{c}(t,t)$ and $I_0(x)$ is the zeroth-order modified Bessel function of the first kind.

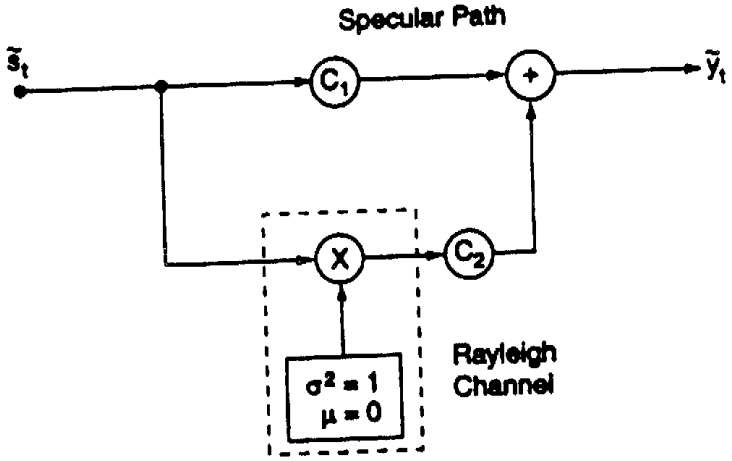

Fig. 2. Simulation model of a Ricean channel

3.4. Statistical Characterization: The WSSUS Model

The time-varying nature of the channel $\tilde{c}(t,t)$ is mathematically modeled as a wide-sense stationary (WSS) random process in *t* with an autocorrelation function

$$R_{\tilde{c}}(t_1,t_2,\Delta t) = E[\tilde{c}^*(t_1,t),\tilde{c}(t_2,t+\Delta t)]$$

In most multipath channels, the attenuation and phase shift associated with different delays can be assumed uncorrelated; this is the *uncorrelated scattering* (US) assumption, which leads to

$$R_{\tilde{c}}(t_1,t_2,\Delta t) = R_{\tilde{c}}(t_1,\Delta t)\, d(t_1 - t_2)$$

The equation above embodies both the WSS and US assumptions, and is referred to as WSSUS model for fading. This autocorrelation function is denoted by $R_{\tilde{c}}(t,\Delta t)$.

The WSSUS model can be presented in the frequency domain by performing a Fourier transform on one or both of the variables *t* and *t*. We obtain this model by Fourier transforming the autocorrelation function in the *Dt* variable

$$S(t,n) = F_{\Delta t}[R_{\tilde{c}}(t,\Delta t)] = \int_{-\infty}^{\infty} R_{\tilde{c}}(t,\Delta t) e^{-j2pn\Delta t} d\Delta t$$

S(t, n) is called the *scattering function* and is perhaps the most important statistical measure of the random multipath channel. From the scattering function we can obtain some of the most important relationships of a channel which impact the performance of a communication system operating over that channel. *The delay-power profile*, sometimes also related to as the *multipath intensity profile, p(t)* is defined as

$$p(t) = R_{\tilde{c}}(t,0) = E\left|\tilde{c}(t,t)\right|^2$$

and presents the average received power as a function of delay *t*.

Another function that is useful in characterizing fading is the *Doppler power spectrum*, which is derived from the scattering function through

$$S(n) = \int_{-\infty}^{\infty} S(t,n)dt$$

3.5. Structural models for Multipath Fading Channels

3.5.1. Diffuse Multipath Channel Model

In some mobile radio channels and some other radio channels such as troposcatter channels the received signal consists of a continuum of multipath components. For mobile radio such channels can be caused by scattering and reflections from very large terrain features such as mountain ranges. This channel type is called *diffuse multipath channel*.

The complex lowpass-equivalent impulse response for the diffuse multipath channel is given by

$$\tilde{c}(t,t) = a(t,t)e^{-j2pf_c t}$$

The received lowpass-equivalent signal is given by

$$\tilde{y}(t) = \int_{-\infty}^{\infty} \tilde{s}(t-t)\tilde{c}(t,t)dt$$

We will assume that the input to the channel is bandlimited to a bandwidth *B*. We can therefore represent the lowpass input in terms of its sampled values using the minimum sampling rate of B samples per second as

$$\tilde{s}(t-t) = \sum_{n=-\infty}^{\infty} \tilde{s}(t-nT)\text{sinc}(B(t-nT))$$

where $T = 1/B$ is the sampling period.

The received signal can be stated as

$$\tilde{y}(t) = \sum_{n=-\infty}^{\infty} \tilde{s}(t-nT)\tilde{g}_n(t)$$

where

$$\tilde{g}_n(t) = \int_{-\infty}^{\infty} \tilde{c}(t,t)\text{sinc}(B(t-nT))dt$$

By examining these equations, we can make some observations:

1. The function $\tilde{y}(t)$ can be generated by passing $\tilde{s}(t)$ through a *tapped delay line* (TDL) with taps $\tilde{g}_n(t)$ spaced *T* second apart.
2. If the impulse response has length *NT*, then $\tilde{g}_n(t)$ will essentially be negligibly small for $n < 0$ and $n > N$ if we assume the integral is dominated by the main lobe of the sinc function. Therefore

$$\tilde{y}(t) = \sum_{n=0}^{N} \tilde{s}(t-nT)\tilde{g}_n(t)$$

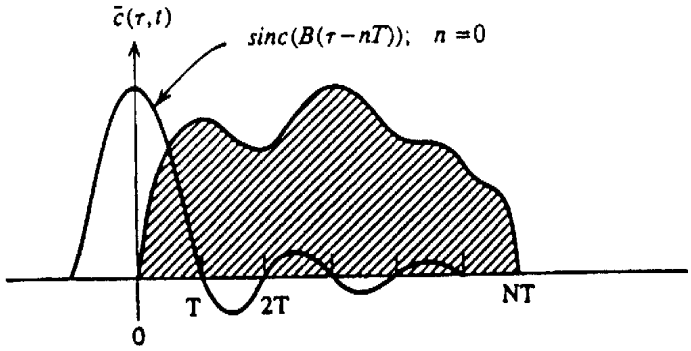

Fig. 3. Illustration of the integration process for obtaining the tap gains of the TDL model

3. Since sinc(Bt) is the impulse response of an ideal filter with bandwidth *B/2*, $\tilde{g}_n(t)$ can be viewed as the filtered version of the channel impulse response sampled at multiples of *T*. If we assume that $\tilde{c}(t,t)$ is fairly smooth over *T*, then $\tilde{g}_n(t)$ can be approximated by

$$\tilde{g}_n(t) \approx T\tilde{c}(nT,t)$$

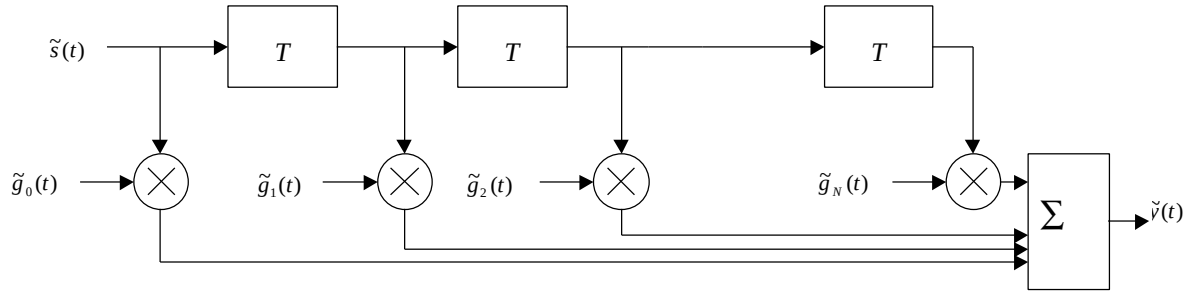

Fig. 4. TDL model for diffuse multipath channels

a. Uncorrelated Tap-Gain Model

A channel cannot have an internal bandwidth constraint and be a WSSUS channel. However, the effect of a WSSUS on a bandlimited signal will be unchanged if the channel is preceded by an ideal bandpass filter having a bandwidth no smaller than *B*.

The simulation model is considerably simplified if we assume that the tap gains are uncorrelated, i.e. $R_{kl}(\Delta t) = 0$ for $k \neq l$. The degree to which R_{kl} is near to zero for $k \neq l$ will depend on the specific nature of $R_{kl}(t, Dt)$. In the approximate case we have

$$E[|\tilde{g}_n(t)|^2] = T^2 E[|\tilde{c}(nT,t)|^2] = T^2 p(nT)$$

where *p(nT)* is the power delay profile. Since $\tilde{g}_n(t)$ is zero-mean complex Gaussian process, we can write $\tilde{g}_n(t) = g_{n,r}(t) + jg_{n,i}(t)$, where $g_{h,r}$ and $g_{n,i}$ are both real Gaussian processes.

The utility of the uncorrelated-tap-gain assumption from the simulation standpoint is that each tap can be independently generated with Gaussian RNG.

After all, there is no single "correct" model since the real channel impulse response depends on many physical variables, and the measurement of the channel response is typically an average of many measurements.

b. Correlated Tap-Gain Model

Without approximation above, the tap-gain functions will be correlated and the channel is now characterized by the covariance matrix

$$\boldsymbol{R}(\Delta t) = \begin{bmatrix} R_{00}(\Delta t) & R_{01}(\Delta t) & \cdots & R_{0N}(\Delta t) \\ R_{10}(\Delta t) & R_{11}(\Delta t) & & R_{1N}(\Delta t) \\ \vdots & & & \\ R_{N0}(\Delta t) & & & R_{NN}(\Delta t) \end{bmatrix}$$

where the average power of tap m is $2\sigma^2 = R_{mm}(0)$.

Generating a set of correlated random processes with an arbitrary covariance matrix is very difficult. Here, not only do we have to generate each $\tilde{g}_n(t)$ in accordance with its specified $R_{nn}(Dt)$, but at the same time do so to satisfy all cross-covariances $R_{kl}(Dt)$ for all k, l.

3.5.2. Discrete Multipath Channel Model

If a multipath channel is composed of a set of discrete resolvable components that originate as reflections or scattering from small structures (houses, small hills) it is called a discrete multipath channel. The model in its most general form has, in addition to variable tap gains, variable delays and a variable number of taps. This model is applicable mostly to rapidly changing environment.

The lowpass-equivalent impulse response of a discrete multipath channel is given as

$$\tilde{c}(t,t) = \sum_{k=1}^{K(t)} \tilde{a}_k(t_k(t),t)\, d(t - t_k(t))$$

with the corresponding lowpass-equivalent output

$$\tilde{y}(t) = \sum_{k=1}^{K(t)} \tilde{a}_k(t_k,t)\tilde{s}(t - t_k(t))$$

For many channels it can be assumed as a reasonable approximation that the number of discrete components is constant and the delay values vary very slowly and can also be assumed constant. The model then simplifies to

$$\tilde{c}(t,t) = \sum_{k=1}^{K} \tilde{a}_k(t)\, d(t - t_k)$$

with the lowpass-equivalent output

$$\tilde{y}(t) = \sum_{k=1}^{K} \tilde{a}_k(t)\tilde{s}(t - t_k)$$

and is also represented as a tapped delay line, as shown in fig. 5.

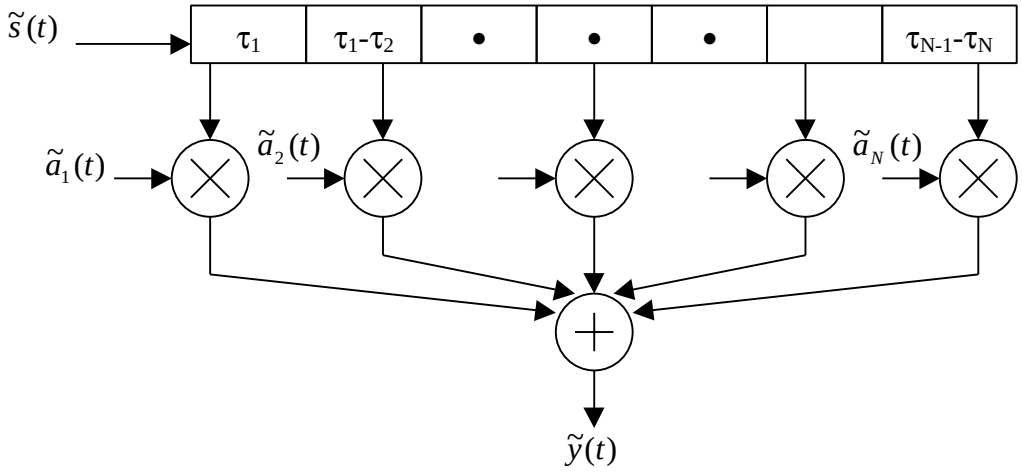

Fig. 5. A variable delay TDL model for discrete multipath channels

Filtered Discrete Channel Models for Simulation

The simulation of the discrete model is quite straightforward. However, sometimes straightforward modeling may result in inefficient simulation. It is advantageous to bandlimit the channel by design to obtain better simulation properties, namely a uniformly spaced tapped delay line.

Applying the bandlimiting method, we obtain the tap gains of uniformly spaced TDL

$$\tilde{g}_n(t) = \int_{-\infty}^{\infty} \tilde{c}(t,t)\mathrm{sinc}(B(t-nT))dt$$

Substituting the impulse response of the discrete channel yields the tap gains

$$\tilde{g}_n(t) = \sum_{k=1}^{K} \tilde{a}_k(t)\mathrm{sinc}(B(t_k - nT)) = \sum_{k=1}^{K} \tilde{a}_k(t)a(k,n)$$

where, with $T = B^{-1}$

$$a(k,n) = \mathrm{sinc}\left[\frac{t_k}{T} - n\right]$$

The $a(k, n)$ decrease quite rapidly. Therefore, the number of taps needed by the bandlimited model is usually small. One way to determine the number of taps is to estimate the bandlimited delay power profile and determine the maximum delay power spread T_m at which the magnitude of the delay spread is still relevant.

The generation of the tap-gain process for the discrete channel model is straightforward. We start with a set of K independent, zero-mean, complex Gaussian white noise processes that are filtered to produce the appropriate Doppler spectrum, then scale them to produce the desired amplitude (average power) of the discrete channel components and transform them using equation for $\tilde{g}_n(t)$ to produce the bandlimited tap gains.

3.6. Indoor Wireless Channel

In the case of indoor wireless channels the number of rays contributing to the total receiver power is much larger than in mobile wireless channel due to the fact that rays in the horizontal plane usually undergo multiple reflections and transmissions at interior or exterior walls of

buildings as well as reflection off furniture. Rays in the vertical plane may also experience multiple reflections at ceilings and floors and may also bounce off furniture.

The distinction between shadow fading and multipath fading is not as appropriate in the indoor channel due to the confined environment and the much lower speed of the mobile. Because of the relatively low speed of the mobiles it is appropriate to develop models that are location-specific, depending only on whether a location is line-of-sight (LOS) to the transmitter or shadowed.

Typical models for indoor wireless channels:

- factory and open-plan-buildings model;
- office building model;
- ray-tracing prediction model.

3.7. Radio-Relay LOS Discrete Multipath Fading Channel Model

The channel is a line-of-sight (LOS) radio channel where the multipath fading is caused by stratification of the atmosphere under certain conditions. Because of the use larger antennas, the field of view of the antenna is limited to very small angles of arrival, and hence the smaller number of multipath components. Also, since the antennas are fixed, the only time variations in the channel characteristics are due to changes in the atmospheric conditions. These variations can be considered very slow compared to the channel bandwidth, which will be on the order of tens of MHz. Hence, the Rummler model is a multipath model with very slow fading. Measured data were used to obtain the values and statistical characterization of the model parameters.

Given the geometry of the link and antenna parameters, Rummler hypothesized a three-ray model of the form

$$y(t) = s(t) + as(t - t_1) + bs(t - t_2)$$

where s(t) and y(t) are the bandpass input and output, respectively. In terms of the complex envelopes, the model takes the form

$$\tilde{y}(t) = \tilde{s}(t) + a\tilde{s}(t - t_1)e^{-j2pf_c t_1} + b\tilde{s}(t - t_2)e^{-j2pf_c t_2}$$

The lowpass-equivalent transfer function of the channel is given by

$$H(f) = 1 + ae^{-j2p(f_c - f)t_1} + be^{-j2p(f_c - f)t_2}$$

On the assumption that over the bandwidth of interest one has $Bt_1 << 1$, which causes frequency nonselective (flat) fading, we can write

$$H(f) = 1 + a + be^{-j2p(f_c - f)t_2}$$

This equation has three random parameters, a, b and t_2.

Typical amplitude and delay responses for Rummler's LOS fading channel model are shown in fig. 6.

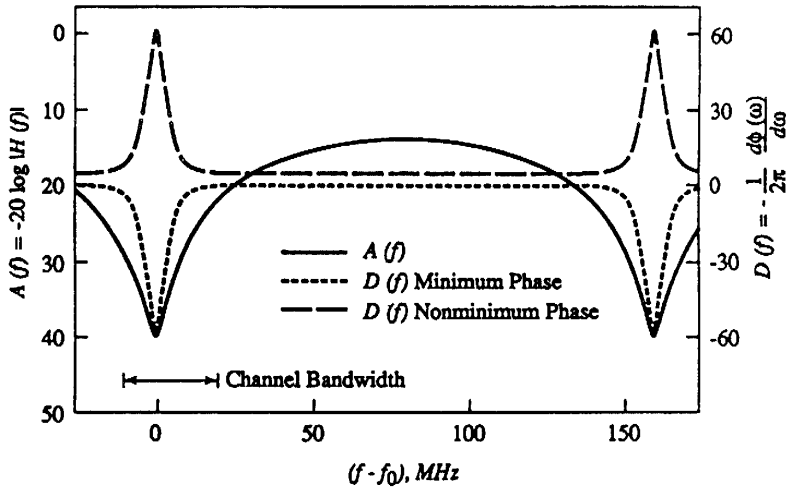

Fig. 6. Typical amplitude and delay responses for Rummler's LOS fading channel model

4. The Almost Free-Space Channel

4.1. Clear-Air Atmospheric Channel

In a clear-air atmosphere, an electromagnetic wave interacts with the oxygen an water vapor that are present in a way that depends on the frequency of the wave. At certain frequencies there are resonances, resulting peaks of absorption.

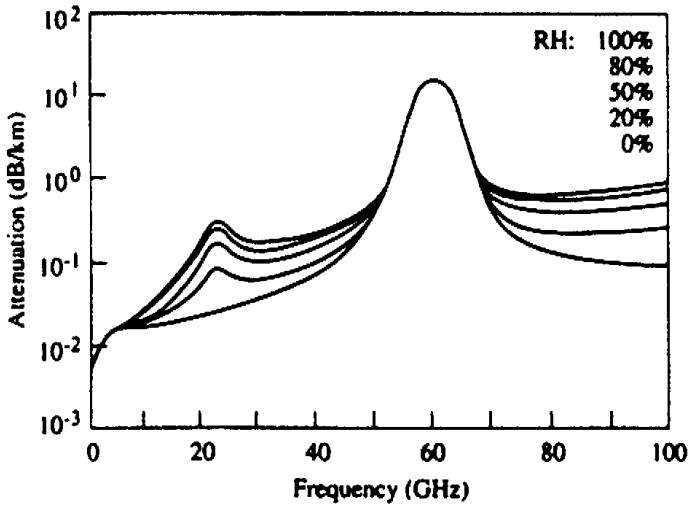

Fig. 7. Atmospheric absorption at sea level as a function of frequency and relative humidity

For analytical analysis the Liebe's model can be used

$$H(f) = H_0 e^{j0.02096\, f\,(10^6+N)L}$$

where N is the complex refractivity in parts per million (in a function of f), $N=N_0+D(f)+jN''(f)$; H_0 is a constant determined from table lookup; N_0 is the frequency-independent refractivity; $D(f)$ is the refractive absorption; $N''(f)$ is the absorption; and L is the distance in kilometers.

4.2. The Rainy-Atmospheric Channel

At microwave frequencies, say above 10 GHz, rain can become a dominant effect on atmospheric propagation. The effect of rain is well known and is usually accounted for as

attenuation which is independent of frequency across the bandwidth of the signal. However, for sufficiently wide bandwidth this attenuation will be frequency dependent, and hence effectively act as a filter.

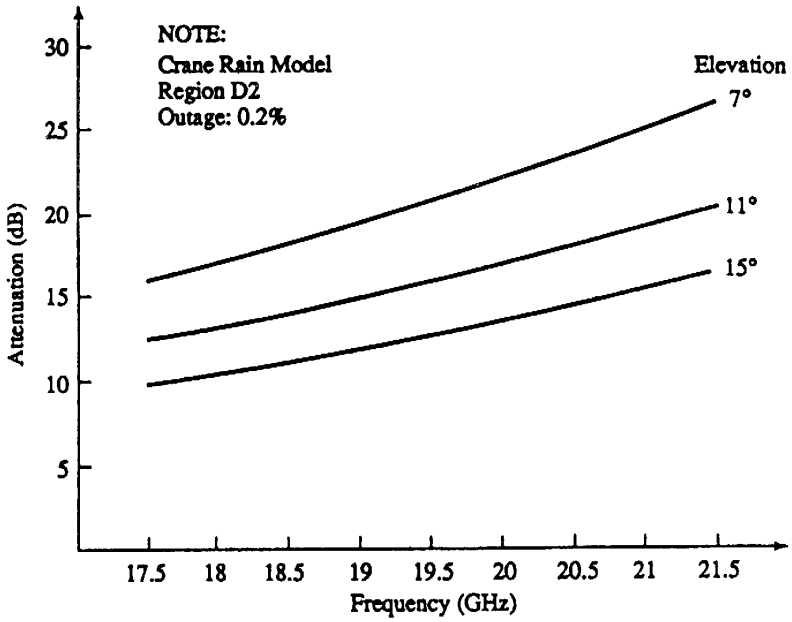

Fig. 8. Rain attenuation as a function of frequency

Another effect of rain, which can be significant in dual-polarized systems, is the depolarization of radio waves. Let

$$S_1(t) = r_1(t)\cos[w_1 t + f_1(t)]$$
$$S_2(t) = r_2(t)\cos[w_2 t + f_2(t)]$$

represents signals of polarization 1 and 2, respectively. The simplest model for depolarization takes the form

$$R_1(t) = a_{11}S_1(t) + a_{21}S_2(t)$$
$$R_2(t) = a_{21}S_1(t) + a_{22}S_2(t)$$

These equations can be generalized by replacing each of the coefficient a_{ij} by a linear frequency-dependent transfer characteristic

$$R_1(t) = h_{11}(t) * S_1(t) + h_{21} * S_2(t)$$
$$R_2(t) = h_{12}(t) * S_1(t) + h_{22} * S_2(t)$$

which is straightforward to simulate if we know the impulse responses h_{ij}(t).

4.3. The Ionospheric Phase Channel

In the lower frequency bands, on the order of a few hundred megahertz and below, the effect of the ionosphere on propagation is extremely complex and best characterized as a time-varying multipath channel. At frequencies above a few hundred megahertz and assuming the absence of anomalous condition (solar flares, nuclear events), an all-pass filter with a nonideal phase characteristic can approximately model the ionosphere. It can be shown hat the phase shift experienced by a wave of frequency *f* due to free electrons in the ionosphere, over and above the free-space propagation lag, is given by

$$f(f) = \frac{2p40\times10^6}{cf}\int_{s_1}^{s_2} N_e(s)ds$$

where c is the speed of light (cm/s), N_e is the areal electron concentration (electrons/cm^2) at any point along the path s, and the integral represents the integrated ("columnar") electron density along the signal path.

5. Conducting and Guided Wave Media

5.1. Rectangular Waveguide Medium

At microwave frequencies, waveguides often serve as the connections between various elements of a system. Since the transfer function is directly proportional to length, the distorting effect may not be negligible.

For rectangular waveguides the transfer function is as follows. The amplitude characteristic $A(f) = 20\log|H(f)|$ is given by

$$A(f) = \frac{a\left[(A/2B)(f/f_c)^{1.5} + (f/f_c)^{-0.5}\right]}{\left[(f/f_c)^2 - 1\right]^{1/2}} \quad \frac{\text{dB}}{\text{m}}$$

where a is a constant depending upon the material and the large dimension; A is the waveguide's large dimension; B is the waveguide's small dimension; f_c is the cutoff frequency, $f_c = c/2A$, where c is the speed of light.

The phase characteristic is given by

$$b(f) = (360/c)f[1-(f/f_c)^2]^{1/2} \quad \text{deg/m}$$

The functions *A(f)* and *b(f)*, multiplied by the waveguide length, can be used directly in simulation.

5.2. The Fiber Optic Channels

Optical pulses propagating along an optical fiber are attenuated and distorted to an extent that depends on the chemical composition of the material used to construct the fiber, as well as on the structure of the fiber. The main distortion is dispersion, of which there are two types, chromatic dispersion and intermodal dispersion. The former describes the effect due to the index of refraction in the fiber, which is nonlinear function of the wavelength – fiber has nonlinear phase characteristic. Intermodal dispersion is an effect that is seen in the multimode fibers, and results from the fact that a large number of ray path lengths are supported by the fiber, generally with different delays.

A mathematical model for the baseband transfer function of an optical fiber can be approximated by

$$H(f) = \int_{-\infty}^{\infty} S(l)L(l)H_{im}(f)H_c(l,f)dl$$

where $S(l)$ is the source spectrum as a function of wavelength; $L(l)$ is the reciprocal of loss; $H_{im}(f)=exp(-s^2_{im}w^2/2 - jwt_d)$ (intermodal dispersion transfer function, normalized to unity gain at

the center frequency); t_d is the fiber time delay; $H_c(l,f)=exp(-jwlT(l))$; l is the fiber length; $T(l)$ is the group delay.

Typical loss curve $L^{-1}(l)$ is shown in fig. 9.

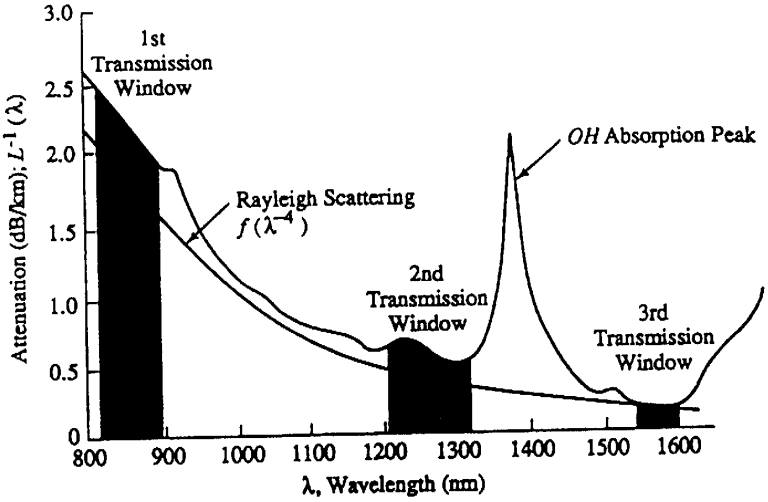

Fig. 9. Typical loss curve as a function of wavelength for an optical fiber

When the width of the source spectrum becomes comparable to the modulation bandwidth, the power domain model becomes inadequate, and a model for the single-mode fiber that assumes linearity in the electric field must be used. The complex lowpass-equivalent transfer function of the fiber is then given by

$$H(f)=\exp\left(-jpd(l_s)\frac{l_s^2}{c}f^2\right)=\exp(-jaf^2)$$

We can recognize that a model of this medium is a parabolic phase filter.

6. Finite-State Model

The terminology “finite-state channel” is used to denote all the elements of a communication system that lie between any two points *a* and *b* in the system where the input entering at point *a* is a symbol sequence $\{X_k\}$ and the output of the system at *b* is another symbol sequence related to the input sequence $\{Y_k\}$. Usually, *a* will be the output of the channel encoder at the transmitter and *b* will be the input to the decoder in the receiver.

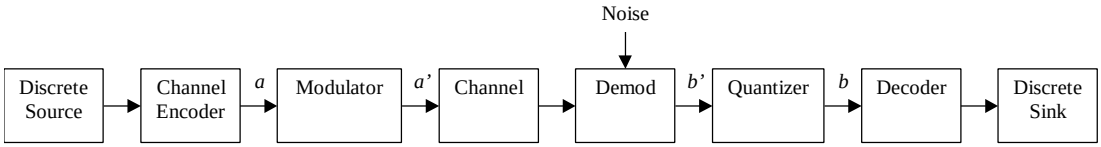

Fig. 10. Definition of a finite-state or discrete channel

In a binary communication system with hard decision decoding, both $\{X_k\}$ and $\{Y_k\}$ will be binary sequences and transmission errors caused by all the elements in between *a* and *b* including the physical channel will cause $\{Y_k\}$ to be different than $\{X_k\}$ at least occasionally.

The nomenclature “finite state” implies a visualization of the channel as being in one of several identifiable conditions, or “states”. The transition from one state to another is governed by some probabilistic rule, which is part of the model. The model description is completed by specifying, for each state, an error generation mechanism.

Finite state channel models fall into two categories. The first category, called *memoryless* models, can be considerate a degenerate case of the general class because such models have only

a single state. Memoryless models are used to model the transmission errors or the transitions from input to the output under the assumption that there is no temporal correlation in the transition mechanism. That is, the probability of transition (or error) for the *n*th input symbol is not affected by what happened to any other input symbol.

The second class of finite-state models are applicable to situations where the transitions from the input symbols to the output symbols are temporally correlated, i.e., the probability of transition for the *n*th symbol is correlated with the transitions of the preceding and/or the following symbols. This will be the case in systems that have fading and impulse noise. Temporal correlation of signal amplitude variations due to fading will cause the transmission errors to be correlated. Errors will tend to occur in bursts and these channels are referred to as *burst error channels* or *channels with memory*.

6.1. Finite-State Memoryless Models

In a finite-state memoryless channel the mapping of input to output is instantaneous and is described by a set of transition probabilities. A standard example of a simple binary memoryless channel model called the binary symmetric channel, is shown in fig. 11.

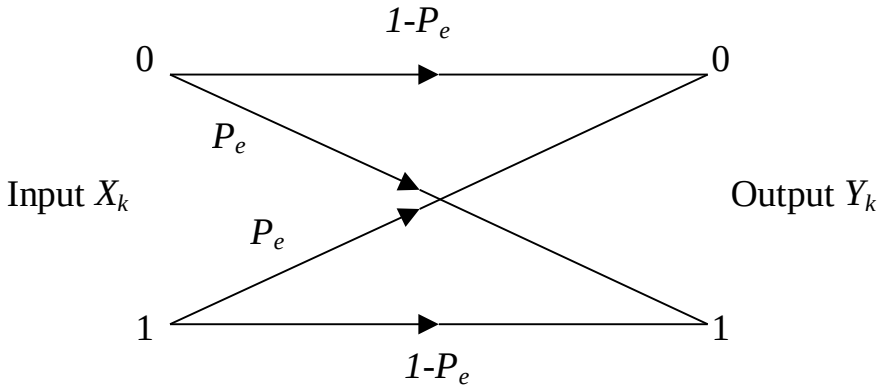

Fig. 11. A simple discrete channel model: the binary symmetric channel (BSC)

The input to the channel is an independent sequence of binary digits $\{X_k\}$ and the output is a binary sequence $\{Y_k\}$. A binary input of "0" is received correctly as "0" with a probability $1 - P_e$ and incorrectly as "1" with an error probability of P_e. The channel is symmetric in that zeros and ones are affected the same way.

A slightly more complicated model for the binary channel is nonsymmetric model for the systems in which the probability of error may be different for zeros and ones, as in some optical communication systems. This model is characterized by a set of input-to-output transition probabilities a_{ij}, $i, j = 0, 1$.

6.2. Finite-State Models with Memory: Hidden Markov Models (HMM)

For channels with memory the most commonly used model is the discrete-time, finite-state Markov model.

To set the stage for Markov models, consider a fading channel in which the received signal strength is above an acceptable threshold part of the time and below the threshold during a deep fade. Ignoring the in-between stages, we can assume the channel to be in either one of the following to "states": (1) a good state in which the received signal level is strong enough that the probability of transmission error for a binary communication system operating over the channel

is almost zero, and (2) a bad state in which the received signal level is so low that the probability of error approaches 0.5. As time progresses, the channel goes from good state to bad state and vice versa. The rate of transition and the length of stay in each of the two states will depend on the temporal correlation of the fading process.

At the beginning of each symbol interval, the channel is one of two states. If the channel is in a good state, then the transmitted bit suffers no transmission error. On the other hand, if the channel is in a bad state, the probability of transmission error is 0.5. Prior to the transmission of each new bit, the channel may change state or remain in the current state. This transition between states takes place with a set of transition probabilities a_{ij}. A graphical representation of the state transition diagram of the model is shown in fig. 11.

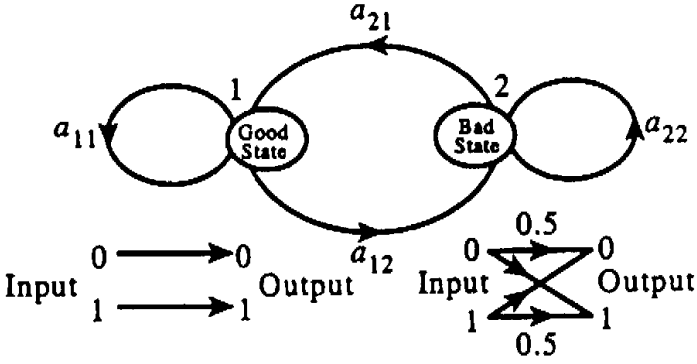

Fig. 12. Example of the state transition diagram for a two-state Markov model

A more general version of the above model can be constructed with a larger number of states, with many good and bad states with varying degrees of “goodness” and “badness”.

An *N*-state Markov model for a discrete communication channel is defined by the following parameters:

- Set of states: {1, 2, 3, …, *N*}.
- State at time $t = S_t$.
- Set of state probabilities:

$p_i(t)$ = probability of being in state i at time $t = P[S_t = i]$, $i = 1, 2, \ldots, N$

- Set of state transition probabilities:

probability of going from state i at time t to state j at time $t + 1$ =

$= a_{ij}(t) = P[S_{t+1} = j \mid S_t = i]$, $i = 1, 2, \ldots, N$

- Set of input-to-output transition (symbol error) probabilities for each state:

error symbols: $E = \{e1, e2, \ldots, e_M\}$; $E = \{1, 0\}$ in the binary case

$b_i(e_k) = P$[error symbol e_k occurring $\mid S_t = i$]

Normally, only the input and the output of the channel and hence the error sequence can be observed, and the state sequence itself cannot be easily observed in a physical channel. Hence, the state sequence is “hidden” or not visible from external observations, and such a Markov model is called a *hidden Markov model* or HMM.

7. Methodology for Simulating Communication Systems Operating over Fading Channels

Consider a typical cellular radio system for voice communication. The performance of the cellular radio interface is usually evaluated at three different levels.

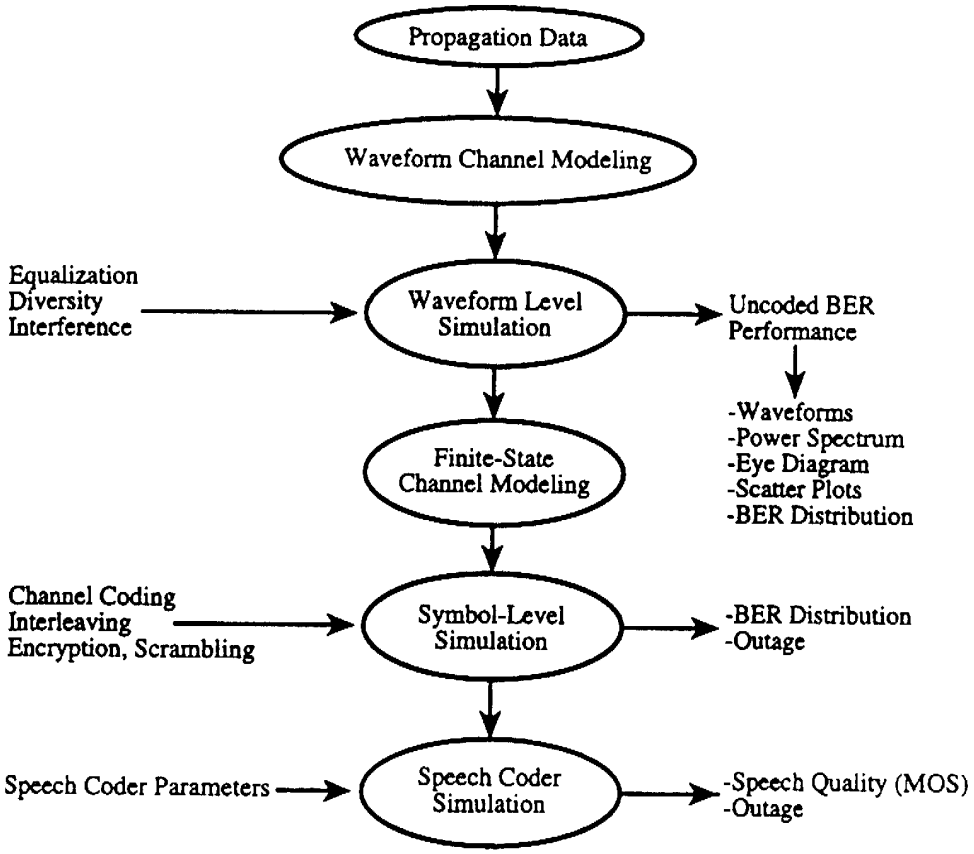

Fig. 13. Organization of the methodology for simulating the performance of a voice communication system operating over a fading channel

At the physical level the performance of the uncoded system is evaluated using a detailed waveform-level simulation. The main objective of this level of simulation is the comparative evaluation of various modulations, and filtering schemes and optimization of system parameters. The output of this level of simulation is the uncoded bit error rate performance and a description of the burst error characteristics of the radio channel including all the effects of waveform level processing blocks such as modulators, filters, and equalizers.

The next level of simulation will be of the coded system using the Markov model. Here, the signal can be more precisely described as a discrete-amplitude, discrete-time sequence. This level is so called symbol level. At the symbol level, comparative performance of coding, interleaving and scrambling schemes are evaluated and the parameters of this portion of the system are optimized.

The third level of performance evaluation deals with the speech coder and the voice quality. This will involve simulating the voice coder with a finite-state channel model for the coded system, and evaluating the voice quality subjectively.

The ultimate measure of performance for voice communication in a cellular radio system is the voice quality as measured by subjective listening tests, which produce a mean opinion survey (MOS). The MOS ranges from 1 to 5, with 5 being an excellent rating. Typically, the quality of service of a cellular radio system will be specified in terms of the requirement that 99% of the time the MOS is better than 2.0.

Reference:

M.C.Jeruchim, P.Balaban, K.S.Shanmugan: Simulation of Communication Systems, 2nd Edition, Plenum Publishers 2000, 924pp.

Problem.

Prove analytically that white Gaussian noise with zero mean and standard deviation σ^2 has the envelope (amplitude) distributed according to Rayleigh distribution and the phase distributed uniformly.

Hint: decompose the noise into sin and cos quadratures and write two-dimensional pdf.